Temperature dependence of $S(Q,\omega)$ in liquid ^{4}He under pressure

E. F. Talbot and H. R. Glyde
Department of Physics, University of Delaware, Newark, Delaware 19716

W. G. Stirling*
Institut Laue-Langevin, 38042 156X Grenoble Cedex, France

E. C. Svensson
Atomic Energy of Canada Limited, Chalk River Nuclear Laboratories, Chalk River, Ontario K0J 1J0, Canada

(Received 13 May 1988; revised manuscript received 15 August 1988)

The temperature dependence of the dynamic form factor, $S(Q,\omega)$, of liquid ^{4}He at $p=20$ bars has been determined by inelastic neutron scattering measurements. Two wave vectors, $Q=1.13$ Å^{-1} and $Q=2.03$ Å^{-1}, corresponding to the maxon and roton regions of the phonon-roton dispersion curve, were studied over a wide range of energy transfer, $\hbar\omega$. Based on previous data at SVP, Woods and Svensson proposed that $S(Q,\omega)$ could be represented as a sum of two components, one proportional to the superfluid density, $\rho_S(T)$, and one proportional to the normal density $\rho_N(T)$. The component proportional to $\rho_S(T)$ contained the sharp one-phonon peak which vanished at $T=T_\lambda$. The aim here is, firstly, to present data on the temperature dependence of $S(Q,\omega)$ at 20 bars and, secondly, to explore whether or not the Woods-Svensson decomposition of $S(Q,\omega)$ holds at higher pressure. At 20 bars and for the Q values investigated here, we find that the sharp peak of $S(Q,\omega)$ does indeed decrease rapidly in intensity as T increases and the corresponding excitation either vanishes or changes abruptly in character at T_λ. The sharp nature of the one-phonon peak T_λ does therefore appear to be associated with superfluidity or a Bose condensate at these Q values. However, the weight of the one-phonon peak does not scale as $\rho_S(T)$ and subtracting a contribution proportional to $\rho_N(T)$ from $S(Q,\omega)$ leads to negative values of the superfluid component of $S(Q,\omega)$ at low ω. Thus $S(Q,\omega)$ at 20 bars does not naturally separate into a part proportional to ρ_S and one proportional to ρ_N. We also explore the consequences of a simple subtraction of the multiphonon component, assumed temperature independent, as an alternative method of extracting one-phonon parameters from the total scattering intensity. The values of the one-phonon properties such as the frequency and the lifetime obtained by the simple multiphonon subtraction method also show a marked change at T_λ.

I. INTRODUCTION

The dynamics of liquid ^{4}He has been investigated[1-4] by inelastic neutron scattering over a wide range of momentum ($\hbar Q$) and energy ($\hbar\omega$) transfer beginning with the pioneering experiments[5-7] of the late 1950's. The dynamic form factor, $S(Q,\omega)$, may be obtained from the observed intensity. For $Q \lesssim 3.6$ Å^{-1} and at low temperatures ($T \approx 1.1$ K), $S(Q,\omega)$ has a single sharp peak at frequency $\omega=\omega(Q)$ superimposed on a wide "multiphonon" continuum. This peak is identified as the collective "phonon-roton" excitation in the fluid density originally proposed by Landau.[8] At low Q ($Q \leq 0.5$ Å^{-1}) most of the scattered intensity is in the one-phonon peak. As Q increases the one-phonon intensity $Z(Q)$ increases until it reaches a maximum in the roton region ($Q \approx 1.92$ Å^{-1} at SVP). The multiphonon intensity continues to grow with Q until it dominates the intensity. At $Q \approx 3.6$ Å^{-1} the sharp peak disappears and for $Q \gtrsim 3.6$ Å^{-1} liquid ^{4}He responds like a gas of weakly interacting atoms. The dynamic form factor $S(Q,\omega)$ is then a broad function peaked slightly below the free-atom recoil energy, $\hbar\omega_R=\hbar^2Q^2/2m$.

The purpose of the present paper is to explore the temperature dependence of $S(Q,\omega)$. In spite of extensive experimental[1-4,9-14] and theoretical[15-20] study, the temperature dependence of $S(Q,\omega)$ is not well understood. The results of Woods and Svensson[11] (WS) suggested that the sharp component of $S(Q,\omega)$ usually identified with one-phonon excitations is unique to the superfluid phase and somehow associated with the existence of a Bose condensate. They also proposed a two-component model for $S(Q,\omega)$ in which the one-phonon peak has a weight proportional to the macroscopic superfluid density $\rho_S(T)$, and hence disappears at T_λ. We are thus led to the following questions: Does the sharp peak in $S(Q,\omega)$ also disappear or change abruptly at the superfluid transition temperature T_λ at higher pressures? Is the weight $Z(Q)$ in the sharp peak proportional to the superfluid density $\rho_S(T)$, as found by WS at SVP? Is $S(Q,\omega)$ also largely independent of T for $T > T_\lambda$? To address these questions we have carried out neutron scattering studies of liquid ^{4}He at $p=20$ bars and several temperatures above and below T_λ. We chose two wave vectors, $Q=1.13$ Å^{-1} and

$Q=2.03$ Å^{-1}, corresponding to the maxon and roton regions of the phonon-roton dispersion curve. The position of the sharp peak [the phonon energy $\hbar\omega(Q)$] is quite different at these two Q values and sits at a quite different position relative to the maximum of the corresponding broad multiphonon background. This difference in position is a help in separating the one-phonon peak from the broad background. Measurements under applied pressure are interesting because the relative weights of the one-phonon and multiphonon components of $S(Q,\omega)$ change significantly with pressure, especially at the maxon wave vector. This offers a test of models of the one-phonon and multiphonon components of $S(Q,\omega)$ under new conditions.

Specifically, Woods and Svensson[11] (WS) proposed that $S(Q,\omega)$ could be expressed as the sum of two components:

$$S(Q,\omega)=\frac{\rho_S(T)}{\rho}S_S(Q,\omega)+\frac{\rho_N(T)}{\rho}S_N(Q,\omega)\ . \tag{1}$$

Here $\rho_S(T)$ and $\rho_N(T)$ are the usual superfluid and normal fluid densities[8,21] of liquid ^{4}He. The $S_N(Q,\omega)$ is a broad normal-fluid component which is essentially the same above and below T_λ. Since $\rho_S(T)$ vanishes for $T>T_\lambda$, $S_N(Q,\omega)$ can be determined from the observed scattering intensity at temperatures immediately above T_λ. The observed intensity above T_λ was found[11] to be nearly independent of temperature for $Q\gtrsim 0.8$ Å^{-1}. Indeed if we write $S_N(Q,\omega)$ as

$$S_N(Q,\omega)=-\frac{1}{n\pi}[n_B(\omega)+1]\chi_N''(Q,\omega)\ , \tag{2}$$

the imaginary part χ_N'' of the dynamic susceptibility χ_N was taken to be independent of T for T above but close to T_λ. In this temperature range all of the observed T dependence in $S(Q,\omega)$ was ascribed to the Bose function $n_B(\omega)=(e^{\beta\hbar\omega}-1)^{-1}$, where $\beta=k_BT$. With χ_N'' assumed independent of T, WS used (2) to determine $S_N(Q,\omega)$ at all T below T_λ. The "superfluid" component $S_S(Q,\omega)$ was taken as the sum of the sharp component (S_1) plus a multiphonon background (S_M),

$$\frac{\rho_S(T)}{\rho}S_S(Q,\omega)=S_1^{\rm WS}(Q,\omega)+\frac{\rho_S(T)}{\rho}S_M(Q,\omega)\ . \tag{3}$$

WS determined $S_S(Q,\omega)$ from the observed $S(Q,\omega)$ via (1) by subtracting out the normal part as

$$\frac{\rho_S(T)}{\rho}S_S(Q,\omega)=S(Q,\omega)-\frac{\rho_N}{\rho}S_N(Q,\omega)\ . \tag{4}$$

They found that the resulting integrated intensity in the one-phonon peak

$$S_1^{\rm WS}(Q)=\int d\omega\, S_1^{\rm WS}(Q,\omega) \tag{5}$$

scaled as $\rho_S(T)/\rho$. This suggested that the one-phonon peak could be identified with the superfluid and that it disappeared at T_λ. WS also found that by associating $\omega(Q,T)$ with the position of only the sharp component $S_1(Q,\omega)$ of $S(Q,\omega)$ they obtained an excitation energy $\omega(Q,T)$ near T_λ that agreed better with the values for elementary excitations inferred from thermodynamic data than energies taken from the whole of $S(Q,\omega)$. The half-width $\Gamma(Q,T)$ of $S_1(Q,\omega)$ also agreed better with the predictions of Landau and Khalatnikov[21] (LK) than did the values obtained from the whole $S(Q,\omega)$, although we would not expect the LK model to hold for T near T_λ where $\Gamma(Q,T)$ becomes large.

A specific aim here is to test whether the WS decomposition (1) holds well at higher pressure; particularly whether the one-phonon intensity $Z(Q,T)$ scales as $\rho_S(T)/\rho$. We argue in the discussion (Sec. VI) that the integrated intensity of the one-phonon peak in (5) as obtained via (3) and (4), *necessarily* scales[20] as $\rho_S(T)/\rho$ if the total $S(Q)$ is independent of T. Since $S(Q)$ is observed to be approximately independent of T, $S_1^{\rm WS}(Q,T)$ defined in Eq. (5) is found to scale as $\rho_S(T)/\rho$. To avoid this issue and to explore the WS decomposition more directly we define the one-phonon intensity $Z(Q,T)$ in terms of $S_1(Q,\omega)$ as

$$\begin{aligned}S_1(Q,\omega)&=-\frac{1}{n\pi}[n_B(\omega)+1]\chi_1''(Q,\omega)\\&=\frac{1}{2\pi}[n_B(\omega)+1]A_1(Q,\omega)\ ,\end{aligned} \tag{6}$$

where

$$A_1(Q,\omega)=2Z(Q,T)\left\{\frac{\Gamma(Q,T)}{[\omega-\omega(Q,T)]^2+\Gamma(Q,T)^2}-\frac{\Gamma(Q,T)}{[\omega+\omega(Q,T)]^2+\Gamma(Q,T)^2}\right\} \tag{7}$$

is the one-phonon response function $[-\chi_1''(Q,\omega)/n\pi=A_1(Q,\omega)/2\pi]$ and $n=N/V$. In (7) we have included both the Stokes $[\omega-\omega(Q,T)]$ and anti-Stokes $[\omega+\omega(Q,T)]$ terms in $A_1(Q,\omega)$. Equation (7) is a direct generalization of the δ function response function

$$A_1(Q,\omega)=2\pi Z(Q,T)\{\delta[\omega-\omega(Q,T)]-\delta[\omega+\omega(Q,T)]\}$$

in which each δ function is represented by a Lorentzian function. Equation (7) is the usual expression for a response function if the real $[\omega(Q,T)]$ and imaginary $[\Gamma(Q,T)]$ parts of the excitation energy are assumed to be frequency independent. As discussed in the Appendix, with both the Stokes and anti-Stokes terms included, (7) is actually identical to the "harmonic oscillator" function often used[12] to describe $S_1(Q,\omega)$. The one-phonon parameters $Z(Q,T)$, $\omega(Q,T)$, and $\Gamma(Q,T)$ are obtained here by fitting this Lorentzian function to $S_1(Q,\omega)$. If the WS decomposition represents the observed $S(Q,\omega)$ well, the $Z(Q,T)$ of (7) should be proportional to $\rho_S(T)/\rho$. [In this paper, both the excitation energy $\omega(Q,T)$ and its width $\Gamma(Q,T)$ will be given in THz.]

A number of authors have attempted to provide a theoretical foundation for the WS formula for $S(Q,\omega)$. Griffin[16] and Griffin and Talbot[17] attempted to recover the WS formula from the microscopic theory based on Bose condensation. They identified the normal-fluid component as scattering from thermal excitations already present in the liquid and associated the superfluid com-

ponent with the creation of one or more quasiparticles (phonons). Griffin and Talbot[17] used the dielectric formalism[22] in a model (one-loop) calculation that neglected the creation of excitations. They found that at low Q the scattering from thermal excitations was indeed roughly proportional to the normal-fluid fraction, but contrary to experiment, the peak in the associated $S(Q,\omega)$ shifted towards higher frequency as the temperature increased. This shift in the peak frequency originated from the dielectric function used in the calculation, a dielectric function involving only thermal scattering and neglecting any one-phonon intermediate states. As this dielectric function clearly played a very important role and also appeared in the one-phonon scattering, it became clear that one-phonon scattering would interfere strongly with the thermal scattering. In a subsequent calculation, Talbot and Griffin[18] included the one-phonon peak and the interference between the one-phonon processes and the thermal scattering, again neglecting the processes where two or more excitations are produced. They argued that the approximations used were reasonable at low Q where the two-phonon scattering is small. The result of this more sophisticated model was a single peak in $S(Q,\omega)$ centered at the one-phonon frequency with a width which scaled roughly as ρ_N, but with no indication of a sharp peak appearing on top of a much broader one.

In the spirit of Kadanoff and Martin,[23] Yamada[19] inverted the two-fluid hydrodynamic equations to obtain the density-density correlation function. He found that one could identify terms proportional to ρ_N/ρ and a resonant term proportional to ρ_S/ρ. He argued that such behavior would extend beyond the hydrodynamic region into the collisionless region. However no proof of this statement was given. Indeed Mineev[20] used a similar approach in the collisionless, but still adiabatic, region ($\tau^{-1} \ll \omega \ll T$) and did not obtain a weight proportional to ρ_S/ρ for the resonant term. Mineev instead attributed the apparent success of the WS formula to the fact that the static structure factor $S(Q)$ changes rather little (5%) between 1 K and T_λ as noted above and discussed further in Sec. VI.

In view of the apparent success of the WS formula at SVP and the difficulty in explaining it, we propose to test it explicitly in liquid ^{4}He at $p=20$ bars. At $p=20$ bars the weight $Z(Q,T)$ of the one-phonon peak is substantially smaller in the maxon region than at SVP. We examine $S(Q,\omega)$ closely at T near T_λ to determine whether the $Z(Q,T)$ vanishes at T_λ. Since both S_N and S_M are broad functions of ω, in practice it can be extremely difficult to separate $S(Q,\omega)$ into different components.

In Sec. II we describe the experiment and present results. In Sec. III the results are analyzed to extract the individual components of $S(Q,\omega)$ defined in Eqs. (1)–(4), (6), and (7). The full $S(Q,\omega)$ given by (1) is reconstructed and compared with the observed $S(Q,\omega)$ in Sec. III. We consider a second (simple) one-phonon extraction procedure in Sec. IV. The one-phonon parameters are presented in Sec. V and a discussion is given in Sec. VI. Finally a discussion of the one-phonon response function (7) is given in the Appendix. Some of the present results have been briefly reported elsewhere.[24]

II. EXPERIMENT AND RESULTS

The measurements of $S(Q,\omega)$ were made using the IN12 triple-axis spectrometer which is situated on a cold-neutron guide tube from the Institut Laue-Langevin high flux reactor. Pyrolytic graphite (002) was used as both monochromator and analyzer. The instrument was operated with a fixed final neutron energy of 1.127 THz (1 THz=47.99 K=4.14 meV), yielding an instrumental resolution of 0.034 THz (FWHM) as measured by the incoherent scattering from vanadium. From this measured elastic resolution, the resolution FWHM at the maxon ($Q=1.13$ Å^{-1}) frequency is calculated to be 0.039 THz and that at the roton ($Q=2.03$ Å^{-1}) frequency is calculated to be 0.036 THz. A cooled (77 K) beryllium filter before the analyzer minimized higher-order scattering contamination.

The high-purity ^{4}He sample was condensed into a 3-cm diam cylindrical aluminum cell in a helium-flow cryostat. The cell contained cadmium discs spaced 1 cm apart vertically to reduce multiple scattering. Sample temperature and pressure were measured by a calibrated carbon resistor and by a Wallace and Tiernan pressure gauge, respectively. For the applied pressure chosen, 20 bars, $T_\lambda=1.928$ K. No *in situ* calibration of T_λ was made, but the quoted temperatures are believed to be reliable to within ± 0.02 K. As well as measuring the temperature dependence of the scattering from the ^{4}He sample, the scattering from the empty cell was determined at 1.27 K. The empty container spectrum, consisting of a sharp elastic peak and a very small flat inelastic background, was subtracted, unadjusted, from the observed ^{4}He scattering to obtain the net scattering from the liquid ^{4}He. The height of the subtracted elastic peak at $Q=1.13$ Å^{-1} is roughly 4200 counts with an integrated intensity of roughly 170 count THz. At $Q=2.03$ Å^{-1}, the height of the elastic peak is roughly 5200 counts with an integrated intensity of roughly 200 count THz. There is then a region near $\omega=0$ (approximately ± 0.04 THz) within which it is not possible to determine accurately the inelastic scattering from the ^{4}He sample.

In Fig. 1 we present the net scattering intensity at the two wave vectors considered, for temperatures below T_λ. As the low temperature one-phonon peak for the roton is so strong, the scale of Fig. 1 does not permit us to see the broad multiphonon component. From Fig. 2, we see, however, that the broad multiphonon component of the scattering at $Q=2.03$ Å^{-1}, $T=1.29$ K lies well above the empty cell background. Figure 3 presents the corresponding spectra at $T=1.9$ K and above $T_\lambda=1.928$ K.

At the lowest temperature in Fig. 1, the spectra consist of a sharp one-phonon component plus a wide multiphonon continuum peak at higher energies. For the maxon wave vector $Q=1.13$ Å^{-1}, the sharp one-phonon peak intensity drops markedly as T increases towards T_λ. While at 1.83 K a small remnant of the sharp component can still be distinguished from the wide multiphonon peak, by 1.90 K this has apparently disappeared. The spectra for the temperatures above T_λ, $T=2.05$, 2.96, 3.94 K are identical to within the experimental uncertainty (Fig. 3). Turning to the spectra at the roton wave vector 2.03

$Å^{-1}$, we see that similar conclusions pertain. Just below T_λ at $T=1.90$ K, a weak-roton signal can still be observed near 0.13 THz. At 1.93 K this seems to have disappeared leaving only a broad scattering intensity which is largely temperature independent. As with the maxon wave-vector scattering, the roton spectra at and not far above T_λ ($T=1.93$, 1.96, and 2.06 K) are indistinguishable (Fig. 3). However, the spectrum at $T=2.97$ K is significantly different with the peak position having shifted to lower frequency and with the peak intensity decreasing somewhat. Although it is not obvious from Fig. 1, close inspection of our results shows that, for both Q values, the high-frequency tail of the distributions (beyond $\nu \approx 0.7$ THz) is, to within experimental uncertainty, completely independent of temperature (see also Fig. 5).

From Figs. 1 and 3 we conclude that at both the maxon and roton wave vectors, the sharp one-phonon component disappears or changes abruptly at or near T_λ. A graphic demonstration of this is provided by Fig. 4 where a two-dimensional projection of the three-dimensional scattering function at the roton wave vector is shown.

III. ANALYSIS FOLLOWING WOODS AND SVENSSON

In applying the Woods-Svensson (WS) model (1) we firstly determined the "normal" scattering component $S_N(Q,\omega)$ by fitting Eq. (2) to the net scattering intensity observed above T_λ shown in Fig. 3. In spite of possible contributions from Rayleigh scattering, we found that a $\chi''_N(Q,\omega)$ in (2) independent of T for $T > T_\lambda$ could readily be identified. The resulting $S_N(Q,\omega)$ for the two Q values are shown in Fig. 5.

Next, the "superfluid" component $[\rho_S(T)/\rho]S_S(Q,\omega)$ at $T < T_\lambda$ defined by (4) was determined by subtracting out the "normal" component $[\rho_N(T)/\rho]S_N(Q,\omega)$ from the observed data points $S(Q,\omega)$. At low ω, we find that the remaining intensity is actually negative for the roton

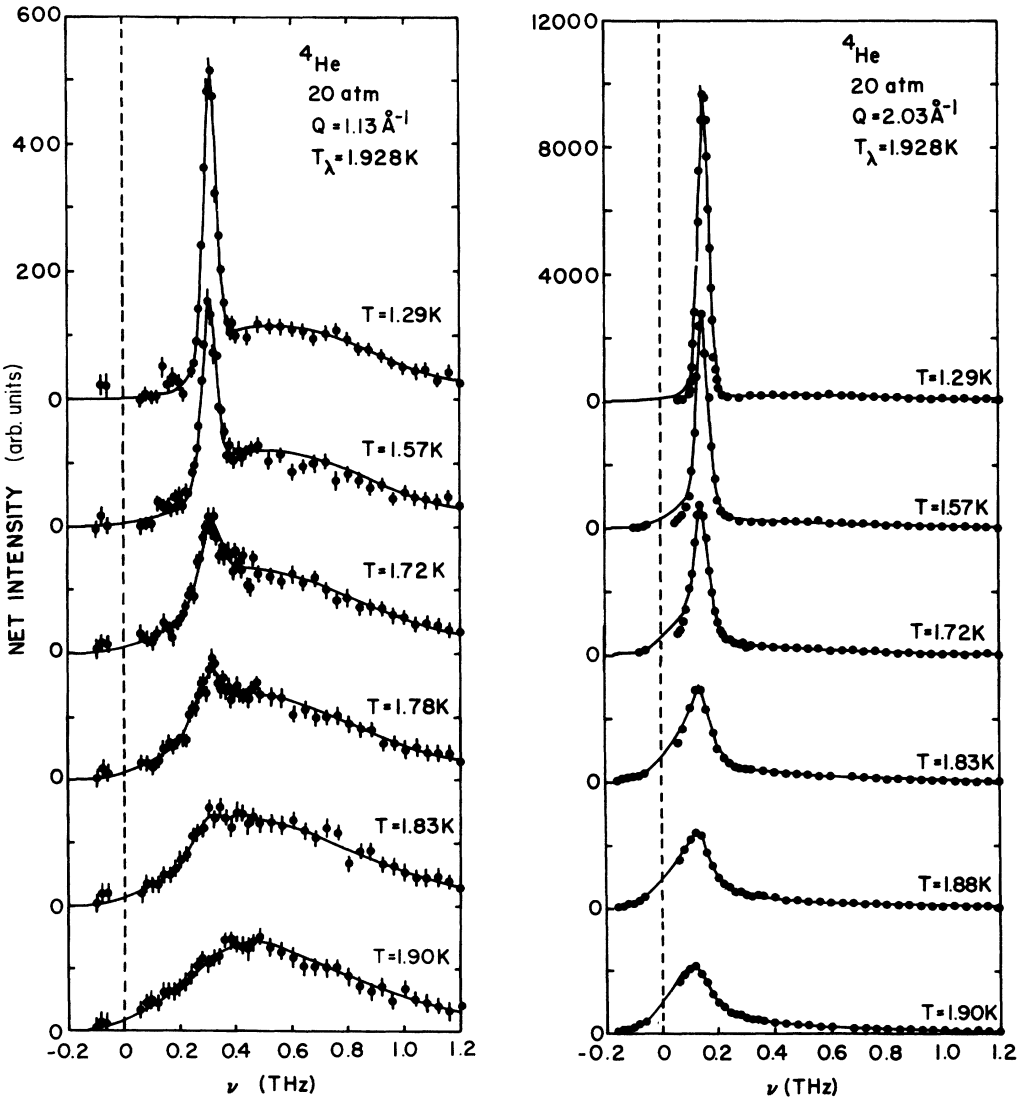

FIG. 1. The net scattering intensities for $T < T_\lambda$ at $Q=1.13$ $Å^{-1}$ and $Q=2.03$ $Å^{-1}$. The solid lines are the Woods-Svensson fit [Eqs. (1)–(7)] to $S(Q,\omega)$. To obtain this fit, $Z^{WS}(Q,T)$ in Eq. (7) is not proportional to $\rho_S(T)/\rho$.

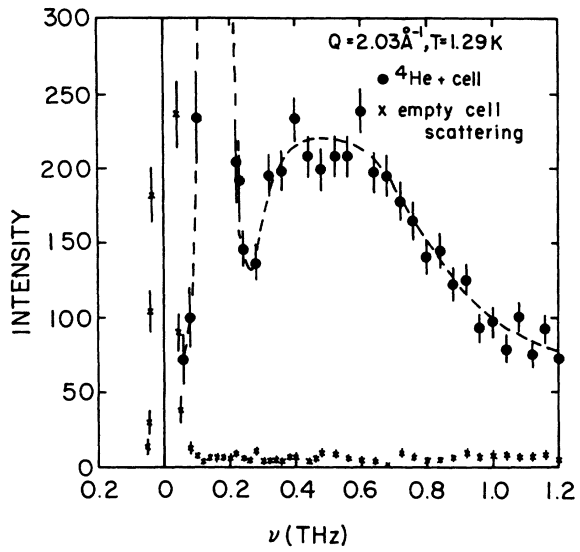

FIG. 2. The raw scattering intensity at $Q=2.03$ Å^{-1}, $T=1.29$ K showing the broad multiphonon scattering (●) (with the dashed line drawn in to guide the eye) and the empty cell scattering (×).

at temperatures $T \leq 1.83$ K. Since a scattering intensity cannot be negative, this shows that at low ω we have subtracted off too much intensity if we assume there is a normal component given by $[\rho_N(T)/\rho]S_N(Q,\omega)$.

Thirdly, at the lowest temperature ($T=1.29$ K), where $[\rho_N(T)/\rho]S_N(Q,\omega)$ is small and the one-phonon scattering is very sharp, we fit (by eye) a broad function to the remaining scattering intensity of (4) to determine the broad multiphonon component $S_M(Q,\omega)$. The resulting $S_M(Q,\omega)$ are plotted as the dashed curves in Fig. 5. At $Q=1.13$ Å^{-1}, the low-frequency end of $S_M(Q,\omega)$ extends into the one-phonon region and it is difficult to separate $(\rho_S/\rho)S_M$ from S_1. We have simply assumed that S_M vanishes at roughly the same frequency as it does at $Q=2.03$ Å^{-1}.

With $S_M(Q,\omega)$ determined and assumed independent of T, we fit the resolution-broadened version of the Lorentzian function given by (6) and (7) to the sharp, one-phonon peak component of $S_S(Q,\omega)$ at all temperatures. Specifically, we assumed that the Bose function $n_B(\omega)$ was negligible in the peak region, that the two Lorentzians in (7) are well separated $[\omega(Q) \gg \Gamma(Q)]$, and that the experimental resolution function was a Gaussian of known width. A single Lorentzian was then convoluted with a Gaussian and the resultant was fitted to the observed peak position, width and height of $S_1(Q,\omega)$ to obtain $\omega(Q)$, $\Gamma(Q)$, and $Z(Q)$, respectively. The resulting fitted values are listed in Table I.

In this way we determine all three components $S_N(Q,\omega)$, $S_M(Q,\omega)$, and $S_1(Q,\omega)$ in the expression (1). The total Woods-Svensson $S(Q,\omega)$ given by (1) and (3), i.e., by

$$S_1(Q,\omega)+\rho_S S_M(Q,\omega)/\rho+\rho_N S_N(Q,\omega)/\rho \ ,$$

can then be reconstructed and this total is shown as the solid lines in Fig. 2(a). The fit is clearly very good except at low ω below the roton peak where $(\rho_N/\rho)S_N(Q,\omega)$ is too large. However we note that the $Z(Q,T)$ determined in this manner does *not* scale as $\rho_S(T)/\rho$ as we discuss below.

IV. SIMPLE MULTIPHONON SUBTRACTION MODEL

In the Woods-Svensson analysis discussed above a normal-fluid scattering function and a multiphonon part of the superfluid scattering function are defined. After subtracting these contributions from $S(Q,\omega)$ we are left with the Woods-Svensson definition of the bare one-phonon scattering from which we can obtain the one-phonon parameters $Z(Q,T)$, $\omega(Q,T)$, and $\Gamma(Q,T)$. Other procedures for obtaining one-phonon parameters have been used by Tarvin and Passell[12] and Dietrich *et al.*[10] Unfortunately both these authors chose to fit a one-phonon scattering function to the *total* scattering although there is a significant multiphonon[25,1] contribution. At the higher temperatures the one-phonon peak is sufficiently wide to have significant overlap with the mul-

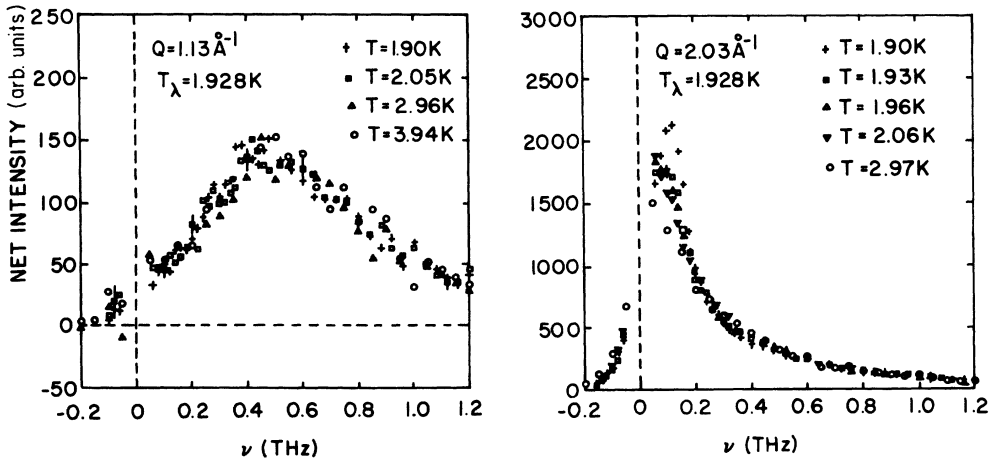

FIG. 3. The net scattering intensities for $T \gtrsim T_\lambda$ at $Q=1.13$ Å^{-1} and $Q=2.03$ Å^{-1}.

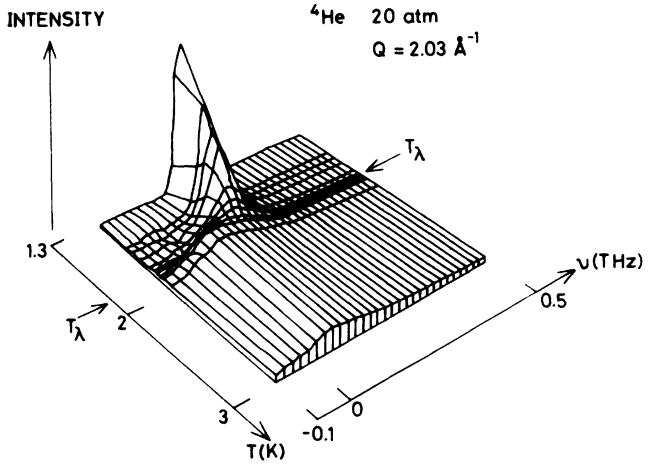

FIG. 4. Temperature dependence of the roton scattering function. The net scattering intensity $S(Q,\omega)$ is plotted vertically. Note the abrupt change of form at or near T_λ.

tiphonon peak. Here some method of separating the multiphonon scattering from the one-phonon contribution must be used to extract meaningful one-phonon parameters. Also, the one-phonon function which Dietrich *et al.* and Tarvin and Passell call a Lorentzian is actually a Lorentzian multiplied by ω. The presence of the ω unfortunately distorts the extracted values of $\omega(Q,T)$ and $\Gamma(Q,T)$ away from those obtained using a normal Lorentzian function. This distortion increases as the groups become wider near T_λ.

In this section we implement the method introduced by Miller, Pines, and Nozières[26] and used by Cowley and Woods[9] to identify the one-phonon and multiphonon contributions at $T=1.1$ K. At this low temperature the one-phonon peak is extremely sharp and, under good resolution conditions, it may be separated[9,25] reasonably unambiguously from the multiphonon contribution. To extend this to higher temperature, we first determine the multiphonon part from our lowest temperature scan ($T=1.29$ K). The resulting multiphonon part $S_M(Q,\omega)$ is identical to the multiphonon part $S_M(Q,\omega)$ defined in (3) and used in the Woods-Svensson analysis (dashed curve in Fig. 5). We then simply subtract (SS) the same $S_M(Q,\omega)$ at each temperature, as if it were independent of T.

Use of a temperature-independent multiphonon part is certainly too simple. Figure 7 of Svensson *et al.*[25] showing $S(Q,\omega)$ at SVP and $Q=0.3$ Å^{-1} shows that the shape of the multiphonon peak can change as T increases to above T_λ. We also know from the study of quantum solids that the two-phonon contribution to $S(Q,\omega)$ increases with T at low ω. By analogy we expect the multiphonon contribution to $S(Q,\omega)$ at low ω in liquid ^{4}He to increase somewhat with T. On the other hand, we find the high-frequency tail of $S(Q,\omega)$ ($\omega \gtrsim 0.7$ THz) is independent of T (as mentioned earlier and see Fig. 1). With these reservations and given that the dominant effect of temperature is to broaden the one-phonon peak, a simple subtraction of a temperature-independent $S_M(Q,\omega)$ should be meaningful. Griffin[27] has already used this method to obtain one-phonon properties at SVP.

This simple subtraction (SS) yields the one-phonon part

$$S_1^{SS}(Q,\omega)=S(Q,\omega)-S_M(Q,\omega) \tag{8}$$

which is to be compared to the WS one-phonon part defined as

$$S_1^{WS}(Q,\omega)=S(Q,\omega)-\left[\frac{\rho_N}{\rho}S_N(Q,\omega)+\frac{\rho_S}{\rho}S_M(Q,\omega)\right]. \tag{9}$$

The S_1^{SS} are depicted in Fig. 6 where we see that most of the high-frequency scattering has been removed. The expressions (6) and (7) are then fitted to $S_1^{SS}(Q,\omega)$. The $S_N(Q,\omega)$ are peaked at lower frequencies than $S_M(Q,\omega)$ and, as a result, the SS one-phonon peak positions are shifted to significantly lower frequencies as T increases to

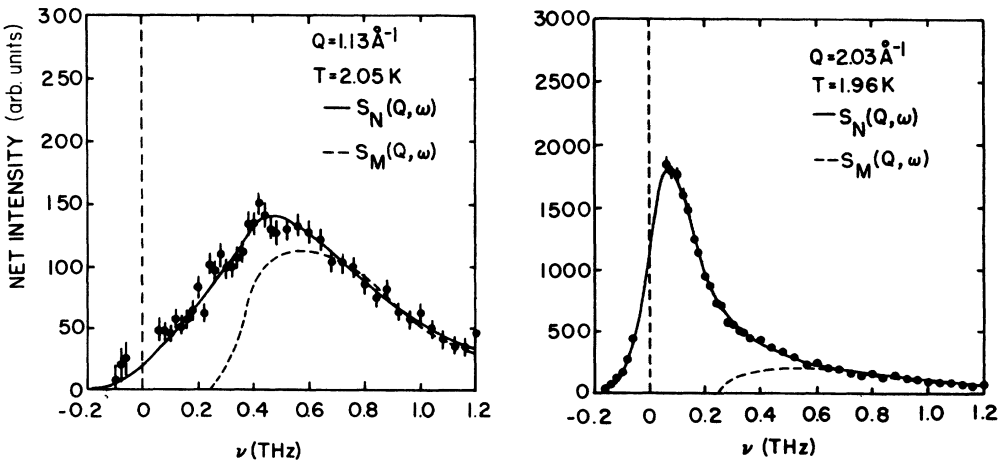

FIG. 5. The normal-fluid component used in the WS analysis for $Q=1.13$ Å^{-1} and $Q=2.03$ Å^{-1}. The dashed curves represent the $T=0$ multiphonon component $S_M(Q,\omega)$.

TABLE I. WS one-phonon parameters.

T (K)	$\omega(Q,T)$ (THz)	$\Gamma(Q,T)$ (THz)	$Z(Q,T)$ (arb. units)
	(a) $Q=1.13$ Å^{-1} (Maxon momentum)		
1.29	0.3102±0.0014	0.0133±0.0025	34.6±2.6
1.57	0.3063±0.0022	0.0178±0.0033	26.2±2.6
1.72	0.3045±0.0035	0.0448±0.0042	24.0±1.8
1.78	0.3002±0.0056	0.0576±0.0061	20.2±2.0
1.83	0.3012±0.0077	0.0754±0.0081	17.1±1.9
1.90	0.294 ±0.025	0.122 ±0.025	10.1±2.6
	(b) $Q=2.03$ Å^{-1} (Roton momentum)		
1.29	0.1537±0.0007	0.0061±0.0014	488±26
1.57	0.1489±0.0007	0.0115±0.0013	410±18
1.64	0.1439±0.0011	0.0156±0.0017	361±20
1.72	0.1418±0.0014	0.0184±0.0021	324±22
1.83	0.1358±0.0014	0.0326±0.0020	228±11
1.88	0.1307±0.0018	0.0340±0.0024	148±9
1.90	0.1299±0.0018	0.0422±0.0024	107±5

near T_λ, particularly at the roton wave vector. For this reason $n_B(\omega)\neq 0$ in the one-phonon region and $\omega(Q,T)$ is not much greater than $\Gamma(Q,T)$ at the higher temperatures. The $Z(Q,T)$, $\omega(Q,T)$, and $\Gamma(Q,T)$ were therefore determined using a least-squares fit to the full expressions (6) and (7). The SS one-phonon parameters are listed in Table II.

V. ONE-PHONON PARAMETERS

In this section, we present the one-phonon parameters $Z(Q,T)$, $\omega(Q,T)$, and $\Gamma(Q,T)$ obtained from the Woods-Svensson model and the simple multiphonon subtraction model.

As described in Sec. III, the WS one-phonon parameters are obtained from fits of Eqs. (6) and (7) to the $S_1^{WS}(Q,\omega)$ defined by (9). Above T_λ the total scattering intensity is simply $S_N(Q,\omega)$; hence from (9) $S_1^{WS}(Q,\omega)$ and therefore $Z(Q,T)$ must vanish at T_λ. The WS one-phonon intensity $Z(Q,T)$ is shown for both the maxon ($Q=1.13$ Å^{-1}) and the roton ($Q=2.03$ Å^{-1}) momenta in Fig. 7. In the upper part of Fig. 7, $Z(Q,T)$ is plotted simply against T. The $Z(Q,T)$ must vanish at $T_\lambda=1.928$ K. Also plotted is $\rho_S(T)/\rho$ scaled to coincide with $Z(Q,T)$ at $T=1.29$ K. Thus even though $\rho_S(T)/\rho$ and $Z(Q,T)$ are fixed to agree at $T=1.29$ K and 1.928 K, we see that there is a significant difference between the observed $Z(Q,T)$ and $\rho_S(T)/\rho$ at intermediate temperatures. This is emphasized further in the lower half of Fig. 7 where we have plotted the WS $Z(Q,T)$ versus $\rho_S(T)/\rho$. We see that the $Z(Q,T)$ exhibit a definite downward curvature showing that there is more scattered intensity immediately below T_λ (small ρ_S/ρ) than predicted by a $Z(Q,T)$ linear in $\rho_S(T)/\rho$.

Figure 8 shows the $Z(Q,T)$ obtained from the SS procedure described in Sec. IV. In this case $Z(Q,T)$ does

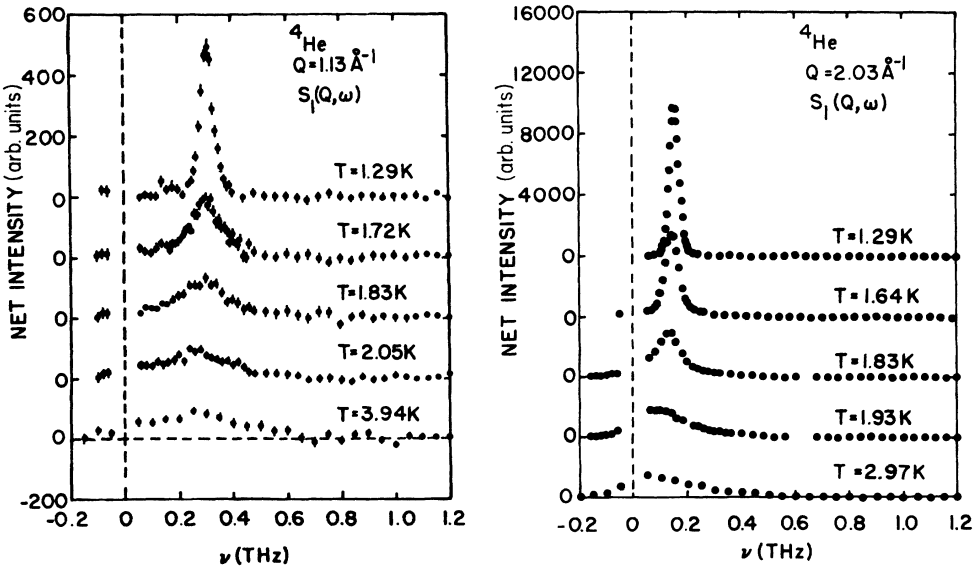

FIG. 6. The simple multiphonon subtraction one-phonon component of the scattering at $Q=1.13$ Å^{-1} and $Q=2.03$ Å^{-1} for several temperatures below and above T_λ.

TABLE II. SS one-phonon parameters. (Error bars are twice the statistical error bars of the fit.)

T	$\omega(Q,T)$ (THz)	$\Gamma(Q,T)$ (THz)	$Z(Q,T)$ (arb. units)	$\pi S_1(q)$ (arb. units)
		(a) $Q=1.13$ Å^{-1} (Maxon momentum)		
1.29	0.3093 ±0.0014	0.0146 ±0.0020	36.2±1.1	35.2±0.9
1.57	0.3043 ±0.0023	0.0296 ±0.0038	34.5±1.4	32.5±1.1
1.72	0.3013 ±0.0048	0.0647 ±0.0087	39.3±2.5	34.5±1.6
1.78	0.2922 ±0.0064	0.086 ±0.012	41.2±3.0	34.6±1.6
1.83	0.285 ±0.013	0.117 ±0.025	47.1±6.3	36.6±2.7
1.90	0.264 ±0.019	0.162 ±0.032	53.7±8.9	36.6±2.6
2.05	0.247 ±0.023	0.176 ±0.042	55±12	35.6±3.0
2.96	0.214 ±0.056	0.194 ±0.070	56±23	34.7±3.9
3.94	0.253 ±0.043	0.200 ±0.069	60±20	42.1±4.6
		(b) $Q=2.03$ Å^{-1} (Roton momentum)		
1.29	0.153 89±0.000 23	0.004 80±0.000 23	474.0±1.4	470.0±1.1
1.57	0.148 42±0.000 31	0.014 00±0.000 38	463.3±1.7	454.9±1.1
1.64	0.143 64±0.000 48	0.019 02±0.000 61	451.6±2.3	440.9±1.4
1.72	0.140 76±0.000 59	0.028 70±0.000 92	490.8±3.6	469.4±2.0
1.83	0.129 9 ±0.001 1	0.055 7 ±0.002 1	545.7±9.8	477.5±3.8
1.88	0.119 0 ±0.001 9	0.078 1 ±0.003 4	628.0±21	489.0±5.4
1.90	0.106 6 ±0.003 5	0.102 1 ±0.004 8	781.0±43	508.5±6.6
1.93	0.074 ±0.011	0.135 7 ±0.007 2	1 210±210	500.6±8.4
1.96	0.058 ±0.015	0.144 9 ±0.007 2	1 590±440	512.0±8.5
2.06	0.002 ±0.015	0.162 1 ±0.003 2	48 000±710 000	517.2±0.9
2.97	0.000 26±0.000 63	0.187 7 ±0.004 1	370 000±920 000	487.5±1.7

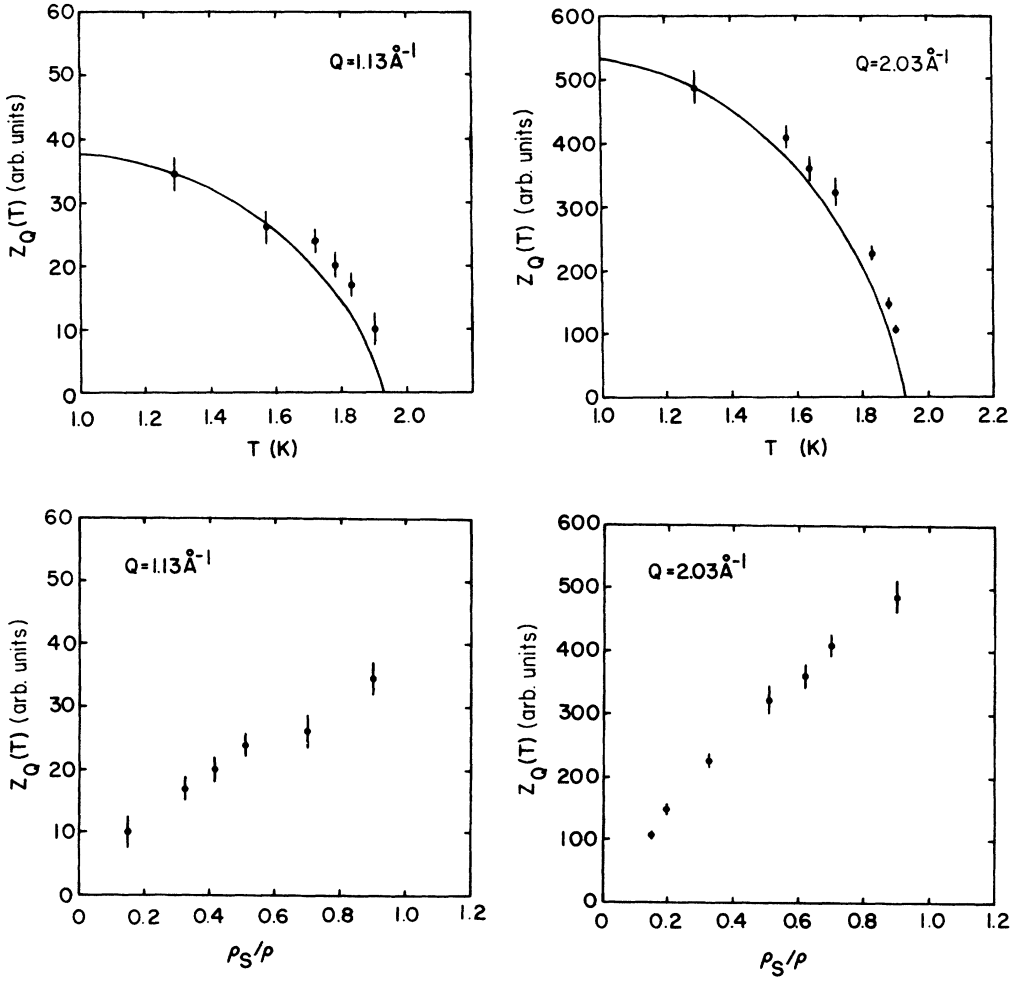

FIG. 7. The Woods-Svensson $Z(Q,T)$ for both $Q=1.13$ Å^{-1} and $Q=2.03$ Å^{-1} plotted vs the temperature (upper part) and vs the superfluid fraction (lower part).

not vanish at $T \gtrsim T_\lambda$. Rather, in the SS method $Z(Q,T)$ stays relatively constant up to $T \simeq 1.8$ K and then increases significantly with T. This final increase near T_λ is a consequence of the definition of $Z(Q,T)$ in (7) and the decrease of $\omega(Q,T)$ with T for $T \gtrsim 1.8$ K. For example, from

$$S_1(Q) = \int_{-\infty}^{\infty} d\omega S_1(Q,\omega)$$

and (6) and (7) we have

$$S_1(Q) \approx \frac{Z(Q,T)}{\pi} \frac{2}{\pi} \tan^{-1} \frac{\omega(Q,T)}{\Gamma(Q,T)} . \quad (10)$$

Since $S_1(Q)$ is approximately independent of T (see Fig. 8 and Table II), $Z(Q,T)$ must increase if $\omega(Q,T)/\Gamma(Q,T)$ decreases. In the SS method, where $\omega(Q,T)$ decreases with T, it might be more appropriate to replace $Z(Q,T)$ by $\tilde{Z}(Q,T)\Gamma(Q,T)/\omega(Q,T)$ in which $\tilde{Z}(Q,T)$ would then be approximately constant. A constant $S_1(Q)$ is really built into the model: If the total intensity $S(Q)$ is approximately independent of T and we subtract a constant multiphonon component $S_M(Q,\omega)$, then the remaining one-phonon intensity $S_1(Q)$ must be approximately independent of T. The SS model therefore requires that the one-phonon component does not "disappear" at T_λ.

Figure 9 shows the one-phonon peak energy $\omega(Q,T)$ and half-width at half maximum $\Gamma(Q,T)$ obtained from both the WS and the SS analysis. The WS analysis, by its definition, only gives one-phonon parameters below T_λ but the SS analysis defines a "one-phonon" component at any temperature. Also shown in Fig. 9 are the peak positions (PP) and half-widths (HWHM) of the full $S(Q,\omega)$ above T_λ.

From Fig. 9 we see the WS $\omega(Q,T)$ for the maxon is essentially independent of temperature while for the roton, $\omega(Q,T)$ decreases by approximately 20% between $T=1.29$ K and T_λ. However the maxon one-phonon peak is very weak and broad near T_λ and it is difficult to determine the $\omega(Q,T)$ accurately near T_λ. By contrast, the SS $\omega(Q,T)$ shows a temperature variation which is about twice as large for $T \leq T_\lambda$. Above T_λ, the simple-subtraction maxon energy flattens off at about 0.25 THz but the best fit to the roton energy goes to zero above $T=1.96$ K.

From the upper part of Fig. 9 we further note that at $T \gtrsim T_\lambda$ the peak position of the total $S(Q,\omega)$ for the maxon ($Q=1.13$ Å^{-1}) is at roughly 0.55 THz, well above either of the WS or SS "one-phonon" energies. This is because the maxon $S(Q,\omega)$ contains significant intensity at high frequency which was subtracted away to obtain the WS or SS one-phonon $S_1(Q,\omega)$. The PP of the total $S(Q,\omega)$ for the roton levels off at roughly 0.08 THz above T_λ.

The WS one-phonon frequencies listed in Table I shows an approximately linear dependence on ρ_S/ρ, a simple consequence of the fact that the temperature dependence of the quasiparticle energies between 1.2 K and T_λ is mainly due to interactions with the rotons. The energy shift is then approximately linear in the number of rotons or ρ_S/ρ. Extrapolating we can obtain the roton energy at $T=0$ K at 20 bars; viz., $\omega(Q,T=0) = \Delta(0) = 0.1575 \pm 0.0010$ THz. As the WS and SS extraction procedures for $\omega(Q)$ are identical and valid at low T, this should be a reliable estimate of $\Delta(0)$.

The lower part of Fig. 9 shows $\Gamma(Q,T)$ as a function of temperature. Also shown for comparison are the half-widths of the total $S(Q,\omega)$ for a few temperatures near and above T_λ and, at the roton momentum, the Landau-Khalatnikov[21] (LK) width of the rotons[28,29] appropriate to $p=20$ bars. For both Q values and from both analyses, $\Gamma(Q,T)$ clearly increases significantly between $T=1.29$ K and T_λ.

At the maxon momentum, the SS $\Gamma(Q,T)$ is consistently about 50% higher than the WS $\Gamma(Q,T)$. Above T_λ, the SS maxon width levels off at roughly 0.2 THz. We note that the total $S(Q,\omega)$ at $T \gtrsim T_\lambda$ has a width which is roughly twice that of the SS "one-maxon" part; again this is a reflection of the fact that our analysis subtracts most of the high-frequency scattering from $S(Q,\omega)$.

At the roton momentum, the WS $\Gamma(Q,T)$ agrees very well with the LK width for rotons.[28,29] In contrast to SVP where WS[11] found that the one-phonon widths

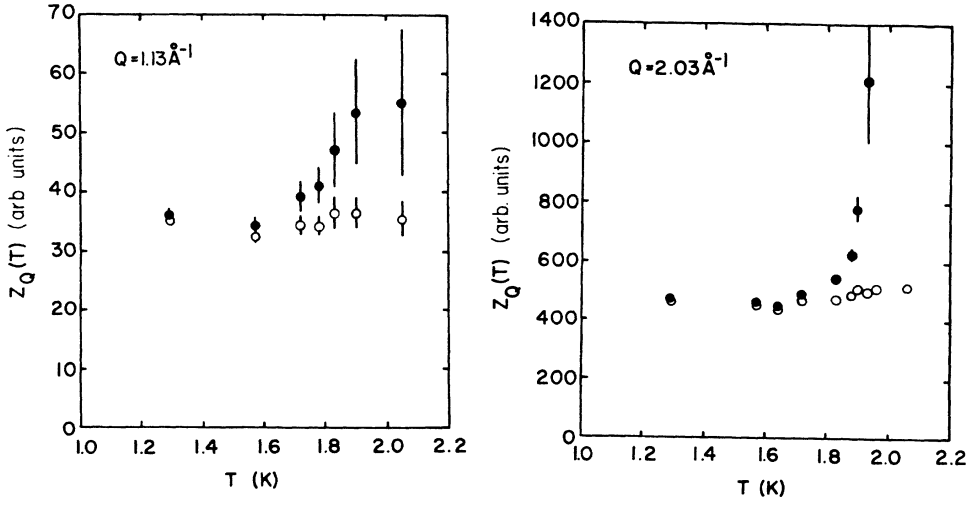

FIG. 8. The simple multiphonon subtraction one-phonon intensities: dots—$Z(Q,T)$; circles—the associated values of $\pi S_1(Q)$.

agreed with the LK result for all Q between 0.8 and 1.93 Å^{-1}, we have found that the maxon width is about twice that of the roton at 20 bars.

Figure 10 shows the variation of the WS widths with temperature on a larger scale. For comparison, we have also included the WS roton widths at SVP[11] and the LK widths[21,28,29] at both SVP and 20 bars. We see that, in contrast with the LK width and the WS widths at SVP, the values of Γ at low temperatures and 20 bars do not go to zero but are significantly greater than their estimated uncertainties. This indicates that, at low temperatures, a mechanism other than roton collisions is determining the quasiparticle width. This is particularly apparent for the maxon where the low-temperature decay mechanisms are probably dominated by the decay of the maxon into two rotons.

The SS $\Gamma(Q,T)$ increases more rapidly than the WS $\Gamma(Q,T)$ as T approaches T_λ, becoming two to three times the WS roton width near T_λ. Above T_λ the SS $\Gamma(Q,T)$ is significantly *larger* than the width of the total $S(Q,\omega)$ for the roton. This is a consequence of the fact that for $T>1.96$ K, the SS $\omega(Q,T)\approx 0$ and

$$Z(Q,T)\omega(Q,T)\equiv\tilde{Z}(Q,T)\Gamma(Q,T)\ , \tag{11}$$

where $\tilde{Z}(Q,T)$ is fairly temperature independent. Under these conditions (7) becomes

$$A(Q,\omega)=\frac{\tilde{Z}(Q,T)}{\pi}\frac{4\Gamma^2(Q,T)\omega}{[\omega^2+\Gamma^2(Q,T)]^2}\ . \tag{12}$$

$\Gamma(Q,T)$ is no longer a good measure of the width of $A(Q,\omega)$; for example, the HWHM of (12) is $\approx 0.74\,\Gamma(Q,T)$. Thus the roton $\Gamma(Q,T)$ for $T>1.96$ K in Fig. 9 are unrealistically large and not very meaningful.

VI. DISCUSSION

The aims of this paper were to determine with high accuracy the temperature dependence of $S(Q,\omega)$ at $Q=1.13$ Å (maxon) and $Q=2.03$ Å (roton), to test the Woods-Svensson (WS) hypothesis at high pressure and to extract one-phonon energies and lifetimes. We obtain estimates of the one-phonon energies and lifetimes in two

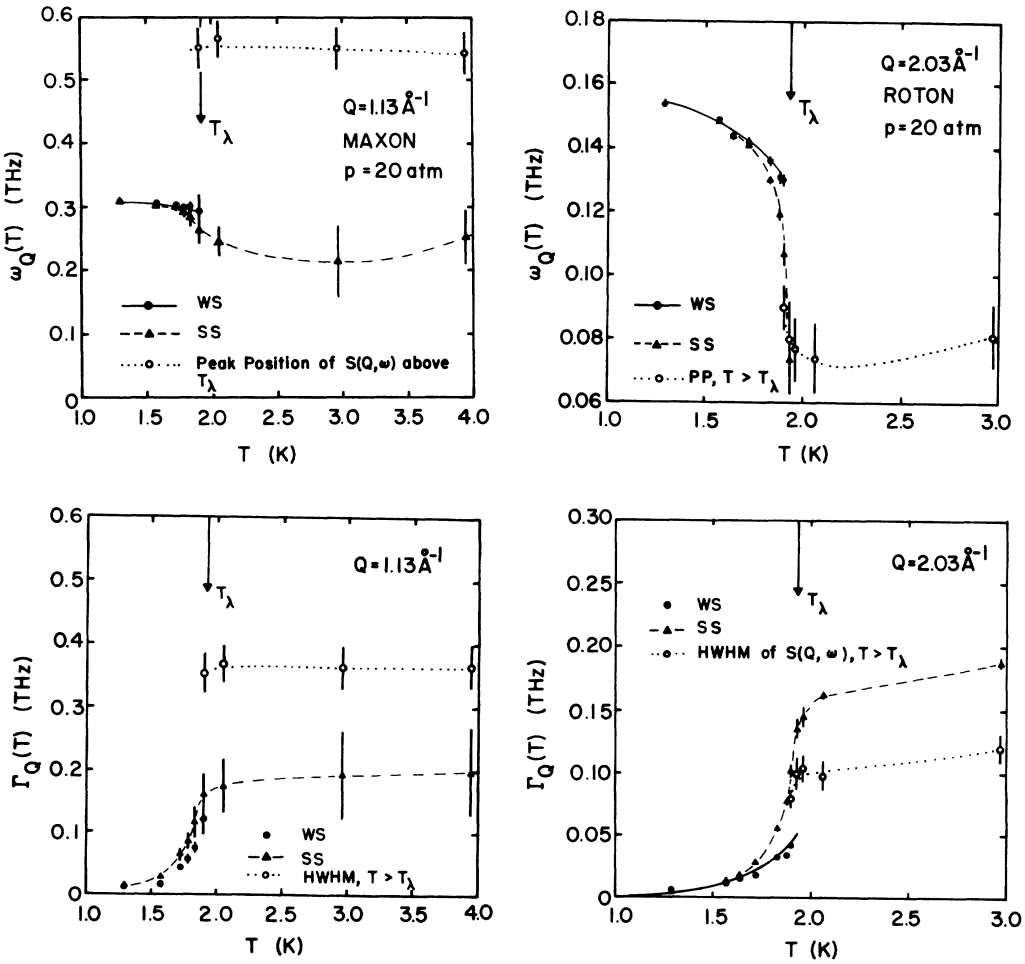

FIG. 9. Upper part: The one-phonon frequencies $\omega(Q,T)$ plotted vs T. Dots—WS analysis; triangles—simple multiphonon subtraction. The open circles denote the position of the center of the total $S(Q,\omega)$ at high temperatures defined as the midpoint of the two half-height points (peak position, PP). Lower part: The corresponding half-widths $\Gamma(Q,T)$ plotted vs T. The solid line at $Q=2.03$ Å^{-1} shows the Landau-Khalatnikov result for the roton width.

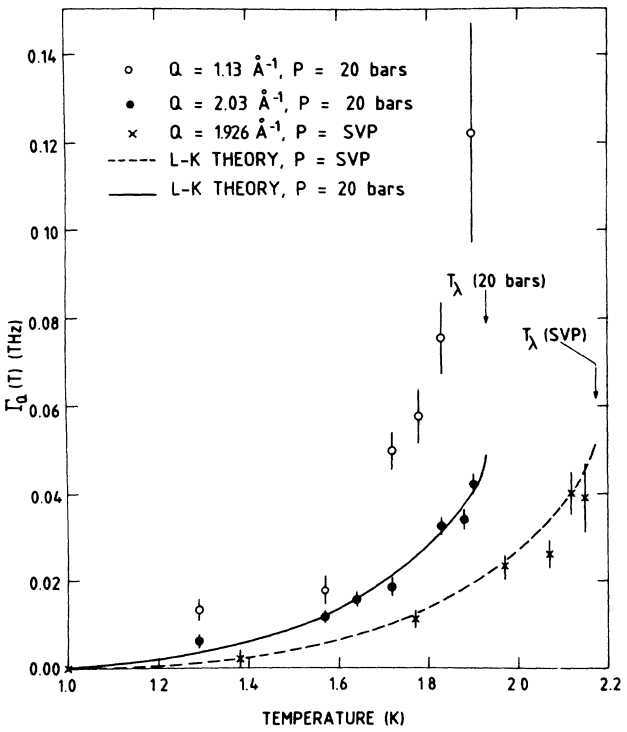

FIG. 10. The WS one-phonon half-widths $\Gamma(Q,T)$ plotted vs T for both $Q=1.13$ Å^{-1} (open circles) and $Q=2.03$ Å^{-1} (solid circles) at 20 bars. Also shown are the SVP roton widths (crosses) and the curves are the Landau-Khalatnikov results for the widths at SVP and 20 bars.

ways. Firstly, a one-phonon part, $S_1^{WS}(Q,\omega)$, of the total $S(Q,\omega)$ was obtained following the WS formula. Secondly, the $T=0$ multiphonon contribution $S_M(Q,\omega)$ was simply subtracted (SS) from $S(Q,\omega)$ at all temperatures as in (8). In both cases, (6) and (7) were fitted to the resulting $S_1(Q,\omega)$ to obtain one-phonon energies $\omega(Q,T)$ and lifetimes $\Gamma(Q,T)$. If $S_N(Q,\omega)$ and $S_M(Q,\omega)$ were the same, then the two methods would yield the same $S_1(Q,\omega)$ since $\rho_N+\rho_S=\rho$. As see from Fig. 5 this is more closely the case for the maxon ($Q=1.13$ Å^{-1}) than for the roton. It is thus not surprising we find that the $\omega(Q,T)$ and $\Gamma(Q,T)$ obtained from the two models are in better agreement for the maxon than for the roton.

A. One-phonon properties

From Fig. 9 we see that for $T\lesssim 1.7$ K the WS and SS methods yield essentially the same $\omega(Q,T)$ and $\Gamma(Q,T)$ for the roton and the maxon. That is, for $T_\lambda - T \gtrsim 0.2$ K the maxon and roton one-phonon peaks are sufficiently sharply defined that the broad component of the scattering can be rather well identified and the remaining one-phonon peak well fitted to (6) and (7) to obtain $\omega(Q,T)$ and $\Gamma(Q,T)$. Within 0.2 K of T_λ, this is no longer true, particularly for the roton. We find $\omega^{SS}(Q,T)$ [$\Gamma^{SS}(Q,T)$] decreases (increases) more rapidly with T than $\omega^{WS}(Q,T)$ [$\Gamma^{WS}(Q,T)$]. Basically this is because a larger fraction of the temperature-dependent background is subtracted in the WS method, leaving a narrower one-phonon peak that changes shape less with temperature. Within 0.2 K of T_λ, it does not appear possible to separate and subtract a multiphonon component unambiguously from $S(Q,\omega)$. Also, the remaining $S_1(Q,\omega)$ is broad enough that fitting (6) and (7) to $S_1(Q,\omega)$ to obtain frequency-independent values of $\omega(Q,T)$ and $\Gamma(Q,T)$ is only approximate. The $S_1(Q,\omega)$ may be a more complicated function of ω than (7), the effective $\omega(Q,T)$ and $\Gamma(Q,T)$ may be ω dependent and $S_1(Q,\omega)$ not describable in terms of a simple "energy" and "lifetime" alone. Thus it could be argued that a one-phonon $\omega(Q,T)$ and $\Gamma(Q,T)$ has meaning up to $T\approx 1.7$ K only.

From Fig. 9 we see that $\Gamma(Q,T)$ increases rapidly with T for $T<T_\lambda$. Indeed at SVP Mezei[13] and Mezei and Stirling[14] find using spin-echo methods $\Gamma(Q,T)\approx 0.01$ K$=0.2\times 10^{-3}$ THz at $T\approx 1$ K for both rotons and phonons. Thus between $T=1$ K and T_λ, $\Gamma(Q,T)$ increases by approximately three orders of magnitude at SVP. For $T\lesssim 1.7$ K we find in Figs. 9 and 10 that $\Gamma(Q,T)$ agrees with the Landau-Khalatnikov[21] result in which $\Gamma(Q,T)\sim\sqrt{T}e^{-\Delta/kT}$, where Δ is the roton energy [$\Delta=\omega(Q,T)$, $Q=2.03$ Å^{-1} here]. Since the LK theory is a perturbation theory using infinite lifetime intermediate state phonons, we do not, however, expect it to hold well when $S_1(Q,\omega)$ is broad, as it is within 0.2 K of T_λ.

Above T_λ, the $\Gamma^{SS}(Q,T)$ and the HWHM of the full $S(Q,\omega)$ are essentially independent of temperature. Thus, if there is a one phonon (zero sound) excitation above T_λ, its damping mechanism is very different from that below T_λ. In this sense there is a very distinct change in the nature of the excitation above and below T_λ as emphasized by Woods and Svensson.[11] The peak position (PP) and HWHM of the total $S(Q,\omega)$ are really the only well-defined quantities above T_λ.

From Fig. 9 we see that $\omega(Q,T)$ also changes markedly at $T\approx T_\lambda$, especially for the roton. For the maxon, the one-phonon frequency [$\omega^{WS}(Q,T)$ or $\omega^{SS}(Q,T)$] lies below the peak positions (PP) of $S(Q,\omega)$ observed above T_λ, i.e., below the PP of $S_N(Q,\omega)$. Since $S_N(Q,\omega)$ and $S_M(Q,\omega)$ are similar (see Fig. 5), the maxon data can be interpreted as a broad multiphonon component, largely temperature independent and centered at $\omega\approx 0.5$ THz, plus a one-phonon component peaked at a lower frequency and which disappears at T_λ. For the roton, the one-phonon $\omega(Q,T)$ lies above the PP of the $S(Q,\omega)$ observed above T_λ, i.e., above the PP of $S_N(Q,\omega)$. In the roton case, however, the broad component centered below $\omega(Q,T)$ grows in intensity with increaing T below T_λ (see Fig. 4). For the roton, both one-phonon and multiphonon intensity are rapidly changing functions of T just below T_λ.

The incremental change in $\omega(Q,T)$ for the roton, $\Delta_0-\Delta(T)\equiv\omega(Q,T=0)-\omega(Q,T)$, is shown in Fig. 11 for $p=20$ atom. There we see that the present values of $\Delta_0-\Delta(T)$ (▲ or ●) are independent of the method of analysis on this scale except immediately below T_λ. These values also lie close to the predictions of Bedell, Pines, and Zawadowski (BPZ)[28] based on a Landau-Khalatnikov-type theory[21] with the coefficients calculated by the solution of a Bethe-Salpeter equation. The short-

dashed line in Fig. 11 is a roton liquid theory[30] (RLT) upper limit to $\Delta_0-\Delta(T)$. However, a roton liquid theory, like a Fermi liquid theory, may not be valid at T near T_λ where the width of the rotons is large. As noted above, a frequency independent $\omega(Q,T)$ and $\Gamma(Q,T)$ may not be meaningful immediately below T_λ.

In Fig. 11 we also show values of $\Delta_0-\Delta(T)$ obtained by Dietrich *et al.*[10] at 20 bars. Their values were obtained by fitting $S(Q,\omega)$ to a Lorentzian function multiplied by ω which we believe is inappropriate. This function, for example, leads to an infinite $S(Q)$ for any finite Γ. Their data agree well with the present data.

At SVP, Tarvin and Passell[12] fitted their roton data to the same Lorentzian multiplied by ω used by Dietrich *et al.*[10] and to a harmonic oscillator (HO) function. The values of $\Delta_0-\Delta(T)$ they obtain at SVP are shown in Fig. 12. As noted above, we believe that the $\Delta_0-\Delta(T)$ values obtained using the Dietrich *et al.*[10] Lorentzian (L) function are too large. In the Appendix we show that the HO function used by Tarvin and Passell (TP) is the same as (7) which we have used. However, in the HO function, they identified the quantity

$$E(Q,T)=[\omega(Q,T)^2+\Gamma(Q,T)^2]^{1/2}$$

as the excitation energy. On the basis of (7) and the discussion in the Appendix, we believe $\omega(Q,T)$ to be the appropriate excitation energy. At low T, where $\Gamma(Q,T)\ll\omega(Q,T)$, $E(Q,T)\rightarrow\omega(Q,T)$. Since $E(Q,T)$ is necessarily larger than $\omega(Q,T)$ the increment $\Delta_0-\Delta(T)\equiv E(Q,0)-E(Q,T)$ obtained by Tarvin and Passell is necessarily smaller. In Fig. 12 we have corrected their $\Delta_0-E(Q,T)$ values to $\Delta_0-\Delta(T)\equiv\omega(Q,0)-\omega(Q,T)$. This raises their HO values for $T\geq 1.9$ K as indicated in Fig. 12 until they lie on the line predicted by Bedell, Pines, and Zawadowski. The corrected TP-HO values then also lie only slightly above those obtained by Woods and Svensson and in reasonable agreement with WS for $T\approx T_\lambda$. This correction from $E(Q,T)$ to $\omega(Q,T)$ as the excitation energy and the rejection of the values (L) obtained using the Dietrich *et al.* Lorentzian removes much of the disagreement in $\omega(Q,T)$ between WS and TP. The TP $\omega(Q,T)$ remain somewhat smaller [$\Delta_0-\Delta(T)$ is larger] because they fitted to the whole of $S(Q,\omega)$ while WS fitted to $S_1(Q,\omega)$ only.

Just above T_λ for $Q=1.13$ Å^{-1}, $S(Q,\omega)$ peaks at 0.5 THz and has a full width at half maximum of $W\approx 0.7$ THz. The corresponding longitudinal phonon group in solid bcc ^{4}He ($p\approx 25$ atom) at $Q\approx 1.0$ Å^{-1} has frequency $\omega_Q\approx 0.6$ THz and $W=0.4$–0.5 THz.[4] Thus $S(Q,\omega)$ in solid helium and liquid ^{4}He above T_λ are similar. In liquid ^{3}He the zero-sound or density component of $S(Q,\omega)$ has $\omega_Q\approx 0.3$ THz and $W\approx 0.15$ THz at $Q=1$ Å^{-1} and $p=10$ atom.[31] The width in ^{3}He is largely independent of T. While energies and widths are smaller in ^{3}He, the shape of $S(Q,\omega)$ is similar in the two normal quantum liquids. This suggests that the nature of the ex-

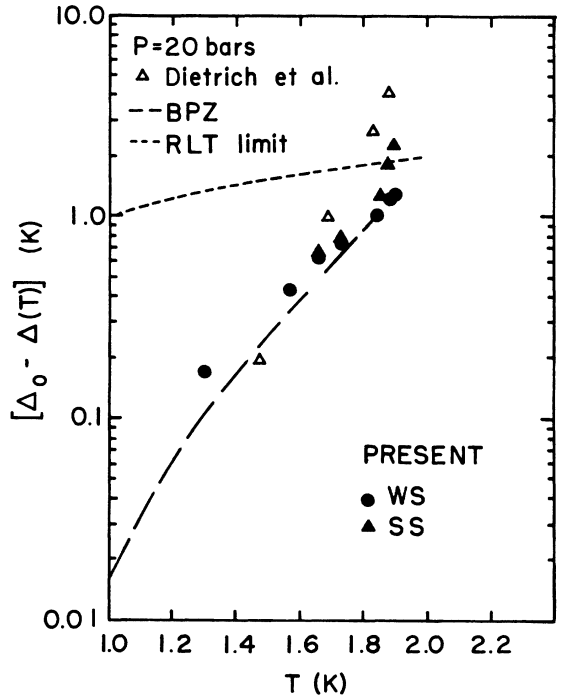

FIG. 11. The shift in the roton gap $\Delta_R(T)$ with temperature at $p=20$ bars as determined by the WS model (solid circles) and the SS model (solid triangles). The Dietrich *et al.*[10] points (open triangles) correspond to fitting the total $S(Q,\omega)$ with a Lorentzian times ω profile function. RLT is the roton-liquid theory upper bound. The Bedell *et al.* (BPZ) calculation is for $p=24.26$ bars.

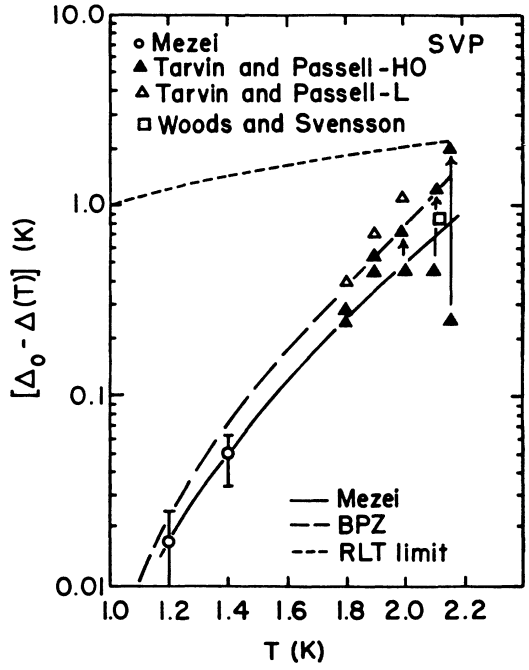

FIG. 12. The shift in the roton gap $\Delta_R(T)$ with temperature at SVP. The solid triangles show the original values quoted by Tarvin and Passell (Ref. 12) and these values corrected upward when $\omega(Q)$ rather than $E(Q)=[\omega^2(Q)+\Gamma^2(Q)]^{1/2}$ is taken as the excitation energy. The open triangles show values obtained fitting a Lorentzian times ω to the total $S(Q,\omega)$. The open circles show Mezei's observed values (Ref. 13) and the solid line his fit to observed values.

citations in normal liquid ^{3}He and ^{4}He and in solid He may be quite similar, namely a damped zero-sound-type phonon mode in the density-density correlation function. Liquid ^{4}He is unique below T_λ, where the one-phonon peak becomes extremely sharp (1000 times sharper than that in the solid or in liquid ^{3}He at $T \approx 1.0$ K) and is rapidly varying with T.

For the two Q's examined here, we find that $S(Q,\omega)$ changes character quite abruptly at T_λ. This agrees with the WS results at SVP. At low Q, $Q \approx 0.2$ Å^{-1}, however, Cowley and Woods observed little change in the full width of the total $S(Q,\omega)$ as T passed through T_λ. Thus while we observe an abrupt change at T_λ for $Q=1.13$ and 2.03 Å^{-1}, this may not be the case at very low Q. We intend to examine this region in detail in a future experiment.

B. Components of $S(Q,\omega)$

In the Woods-Svensson decomposition (1), the one-phonon scattering intensity $Z(Q,T)$ should scale as $\rho_S(T)/\rho$ below T_λ. As noted in Sec. V we find that $Z(Q,T)$ does not scale as $\rho_S(T)/\rho$ at $p=20$ bars. Also, the superfluid component $S_S(Q,\omega)$, obtained from (4), can be negative at small ω which is not physically meaningful. Thus the WS decomposition (1), at least with the temperature dependence given by $\rho_S(T)/\rho$ and $\rho_N(T)/\rho$, does not appear to be precise enough to have fundamental meaning.

WS found that their one-phonon intensity $S_1^{\rm WS}(Q)$ given by (5) scaled as $\rho_S(T)/\rho$ at SVP while we find $Z(Q,T)$ in (7) does not. This difference can be ascribed to a difference in analysis of the data. Their conclusion, as pointed out by Mineev,[20] follows if $S(Q)$ is approximately independent of T. To see this, we note that (3) and (4) imply that the WS one-phonon weight (5) is given by

$$S_1^{\rm WS}(Q)=S(Q)-\frac{\rho_N}{\rho}S_N(Q)-\frac{\rho_S}{\rho}S_M(Q)\ . \tag{13}$$

As $S(Q)$ is found experimentally[32] to be constant to within 5% in the temperature range 1.0 K to T_λ, we have $S_N(Q)\simeq S(Q)$ at all T and (13) becomes

$$S_1^{\rm WS}(Q)=\frac{\rho_S}{\rho}[S(Q)-S_M(Q)]\ , \tag{14}$$

i.e., $S_1(Q,T)$ is proportional to $\rho_S(T)/\rho$ if $S_M(Q)$ is chosen to be temperature independent as WS assumed it to be. Thus we believe that $S_1^{\rm WS}(Q)\propto\rho_S(T)/\rho$ follows from the assumptions of the model and the fact that $S(Q)$ is approximately independent of T in practice. In the present case $Z(Q,T)$ was determined by fitting (7) to the observed $S_1(Q,\omega)$, not by integrating the observed $S_1(Q,\omega)$. We believe that $Z(Q,T)$ in (7) is a better measure of the one-phonon weight.

By contrast, the simple-subtraction model has a one-phonon weight given by

$$S_1^{\rm SS}(Q)=S(Q)-S_M(Q)\ , \tag{15}$$

and, as a consequence, the SS model forces $S_1^{\rm SS}(Q)$ to be essentially independent of temperature. In summary, the assumptions used in each model force the associated one-phonon weights to have certain temperature dependences.

Although the form (1) does not fit well at $Q=2.03$ Å^{-1} and has no theoretical justification, we do find a sharp component below T_λ as pointed out by WS. From this point of view it does make sense to determine $\Gamma(Q,T)$ and $\omega(Q,T)$ by fitting (7) to the sharp component of $S(Q,\omega)$ only, as suggested by WS.

C. Interpretation and summary

We now attempt to interpret our results in terms of existing theories of excitations in liquid ^{4}He. In the original postulates of Landau,[8] the first microscopic description by Feynman[33] and in subsequent theoretical work by Aldrich, Pines, and collaborators,[34] the sharp peak is a collective phonon mode in the density of the liquid. These theories do not make explicit use of a Bose condensate or a broken Bose symmetry. Feynman[33] made explicit use of Bose statistics but not apparently of the condensate fraction. The phonons are very sharply defined at low T because there is a single dispersion curve and decay of a single phonon into two others is severely limited by phase-space requirements. The recent measurements by Mezei and Stirling[14] which show that the line width increases at low Q in the region of upward dispersion in $\omega(Q)$ support this picture. At larger Q, phonon decay is primarily via a four phonon process[21,28] requiring a thermal phonon, scarce at low T. This picture might be expected to hold equally well above as below T_λ. Indeed the measurements of Cowley and Woods for low-Q phonons suggest that the width of $S(Q,\omega)$ continues to increase with T at approximately the same rate above and below T_λ. At $Q \gtrsim 1$ Å^{-1} the WS results and those presented here clearly show that the temperature dependence of $S(Q,\omega)$ is quite different above and below T_λ.

The present results may be interpreted within the dielectric function formulation of $S(Q,\omega)$. This can be traced back to Hugenholtz and Pines[35] who showed that, in a dilute Bose gas having a large n_0, the poles in the single-particle Green's (G) function show up in the total density-density response function (χ). When $n_0=0$, there is no relation between the poles of the two functions. For a strongly interacting Bose fluid such as liquid ^{4}He, where n_0 is small, Gavoret and Nozières[35] showed that below T_λ, χ and G have common poles but there are also additional terms in χ which do not appear in G. More recently, the dielectric formalism developed by Ma and Woo[22] and others has shown that, below T_λ, χ and G each have two poles, denoted $\tilde{\omega}_1$ and $\tilde{\omega}_2$ and that χ and G share a common denominator. This interpretation has recently been reviewed by Griffin.[27] Above T_λ, χ has the usual zero-sound mode of energy $\omega(Q)=\omega_1(Q)$ [the pole of G being denoted as $\omega_2(Q)$]. Below T_λ this $\omega_1(Q)$ is shifted in energy due to the coupling with the single-particle Green's function to $\tilde{\omega}_1(Q)$ and the decay mechanisms can be quite different. Also, below T_λ where $n_0\neq 0$, the $\tilde{\omega}_1(Q)$ becomes a common mode of χ and G and for this reason $\tilde{\omega}_1(Q)$ also becomes an elementary ex-

citation or single-particle mode in the fluid. Payne and Griffin[36] have recently contrasted the dilute Bose gas and strongly interacting Bose fluid characters and discussed the interplay between $S(Q,\omega)$ and the single-particle Green's function in model calculations. The weight of the pole at $\tilde{\omega}_2(Q)$ appears to be very small in χ since it has not been observed.[37] Within this picture, a change in the mode energy and damping mechanism is expected at T_λ. The extent of this change could certainly be a sensitive function of Q—which appears to be the case experimentally.

In summary the present data shows that the one-phonon widths at both Q values increase sharply with T up to T_λ. For $T > T_\lambda$, the HWHM of $S(Q,\omega)$ increases little with T. The details of $S(Q,\omega)$, however, are quite different for the two wave vectors. The maxon frequency $\omega(Q,T)$ decreases little with increasing T for $T < T_\lambda$ while the roton $\omega(Q,T)$ drops significantly. For the maxon, there is a broad multiphonon component which is reasonably independent of T. Thus in Fig. 5, the $S_N(Q,\omega)$ defined by the scattering at $T > T_\lambda$ and $S_M(Q,\omega)$ defined by the low-temperature multiphonon scattering are quite similar at $Q = 1.13$ Å^{-1}. The maxon $S(Q,\omega)$ can, therefore, be reasonably described as a sharp one-phonon component, which disappears at T_λ, superimposed on a reasonably temperature-independent multiphonon background. This is the essence of the WS model. In the SS model, there is a one-phonon component which persists to $T > T_\lambda$ where it is defined as the difference $S_N(Q,\omega) - S_M(Q,\omega) \equiv S_1^{SS}(Q,\omega)$.

The roton behavior is quite different. At $Q = 2.03$ Å^{-1}, the $S_N(Q,\omega)$ is much larger at low ω than $S_M(Q,\omega)$ (see Fig. 5). Thus either the multiphonon background or the one-phonon contribution significantly increases the scattering intensity at low ω as T increases toward T_λ. As seen from Fig. 4, the sharp peak has either become very broad or has vanished at T_λ. However, $S_N(Q,\omega) - S_M(Q,\omega) \equiv S_1^{SS}(Q,\omega)$ is large for the roton for $T > T_\lambda$. The temperature dependence of the intensity of the roton thus remains difficult to interpret.

Finally we reiterate that a necessary consequence of the WS model is that the one-phonon intensity vanishes at T_λ whereas, in the SS model, it must remain essentially constant. The two models are found to agree for $T \lesssim 1.7$ K. Although we have not been able to determine one-phonon parameters for higher temperatures, it is none the less clear from our observed results that there is a marked change in the one-phonon contribution at or very close to T_λ. It either vanishes there or becomes extremely broad.

ACKNOWLEDGMENTS

It is a pleasure to acknowledge the expert technical assistance of D. Marcenac and D. Puschner and valuable discussions with Dr. A. Griffin and Dr. L. Passell. Support from the U.S. Department of Energy, Office of Basic Energy Sciences, under Contract No. DE-FG02-84ER45082 and from a North Atlantic Treaty Organization (NATO) collaboration grant is gratefully acknowledged.

APPENDIX

In this appendix we outline the origin of the response function (7) and relate it to the harmonic oscillator function used by Tarvin and Passell[12] and to the response function for phonons in solids. In this way we attempt to justify (7). For convenience we set $Z(Q,T) = n = 1$.

The zero-order retarded Green's function for a free Bose particle (or phonon) is[38]

$$\chi_1^0(Q,\omega) = G_1^0(Q,\omega) = \left[\frac{1}{\omega - \omega_Q^0 + i\epsilon} - \frac{1}{\omega + \omega_Q^0 + i\epsilon} \right] = \frac{2\omega_Q^0}{(\omega + i\epsilon)^2 - \omega_Q^{02}} . \quad \text{(A1)}$$

Here ω_Q^0 is the energy of the infinitely-lived single-particle excitation. The corresponding response (or spectral) function is

$$A_1^0(Q,\omega) = -2G_1^{0\prime\prime}(Q,\omega) = 2\pi[\delta(\omega - \omega_Q^0) - \delta(\omega + \omega_Q^0)] . \quad \text{(A2)}$$

Clearly the first term (the Stokes term) of $A_1^0(Q,\omega)$ is highly localized around $\omega = \omega_Q^0$ and the second (the anti-Stokes term) around $\omega = -\omega_Q^0$. Taking account of the interaction of the Bose excitation with other particles or excitations,[38] ω_Q^0 acquires a self-energy, $\Sigma_Q(\omega)$, such that

$$\omega_Q^0 \to \omega_Q^0 + \Sigma_Q(\omega) = \omega_Q(\omega) - i\Gamma_Q(\omega) , \quad \text{(A3)}$$

where $\Sigma_Q(\omega) = \Delta_Q(\omega) - i\Gamma_Q(\omega)$ is complex and frequency dependent and $\omega_Q(\omega) = \omega_Q^0 + \Delta_Q(\omega)$. Also $\Delta_Q(\omega)$ and $\Gamma_Q(\omega)$ are even and odd functions of ω, respectively [e.g., $\Gamma_Q(-\omega) = -\Gamma_Q(\omega)$]. The basic approximations made to arrive at (7) are to assume that $A_1(Q,\omega)$ is highly localized around $\omega \simeq \omega_Q$ and $\omega = -\omega_Q$ and to set $\Gamma_Q(\omega) = \Gamma_Q(\omega_Q) \equiv \Gamma_Q$ and $\omega_Q(\omega_Q) = \omega_Q$. Substituting (A3) for ω_Q^0 in (A1), and recognizing that the second term of (A1) is localized at negative $\omega \approx -\omega_Q$ for which $\Gamma_Q(-\omega_Q) = -\Gamma_Q(\omega_Q) = -\Gamma_Q$, we have

$$G_1(Q,\omega) = \left[\frac{1}{\omega - \omega_Q + i\Gamma_Q} - \frac{1}{\omega + \omega_Q + i\Gamma_Q} \right] \quad \text{(A4)}$$

and

$$A_1(Q,\omega) = -2G_1''(Q,\omega) = 2\left[\frac{\Gamma_Q}{(\omega - \omega_Q)^2 + \Gamma_Q^2} - \frac{\Gamma_Q}{(\omega + \omega_Q)^2 + \Gamma_Q^2} \right] . \quad \text{(A5)}$$

The form (A5) and (7) is discussed for quasiparticles by Nozières[39] and for phonons by Ambegaokar *et al.*[40] and Lovesey.[41] Equation (7) should be valid whether the excitation in liquid ^{4}He is interpreted as a quasiparticle or a phonon for small Γ_Q. Equation (7) satisfies $A_1(Q,-\omega) = -A_1(Q,\omega)$.

By combining the Lorentzian functions in (7), we may write $A_1(Q,\omega)$ as

$$A_1(Q,\omega)=\left[\frac{8\omega\omega(Q)\Gamma(Q)}{\{\omega^2-[\omega^2(Q)+\Gamma^2(Q)]\}^2+4\omega^2\Gamma^2(Q)}\right]. \tag{A6}$$

Tarvin and Passell fitted (A6) to their data, calling (A6) the harmonic oscillator (HO) function. We see that the HO function and the symmetrized Lorentzian function (7) are identical. However, Tarvin and Passell identified the sum $E^2(Q)=\omega^2(Q)+\Gamma^2(Q)$ in (A6) as the excitation frequency squared. We believe from (7) that it should be $\omega^2(Q)$. Certainly, since WS used only the first term of (7) to fit their data, for the WS and TP excitation energies to agree beginning with identical data, we must interpret $\omega(Q)$ as the excitation energy in each case. As noted in connection with Fig. 12, a large part of the difference between the HO excitation energies of TP and those of WS at SVP arose because TP used $E^2(Q)=\omega^2(Q)+\Gamma^2(Q)$ while WS used $\omega^2(Q)$.

.Equation (7) and the HO function (A6) may also be obtained by analogy with phonons in a solid. From Dyson's equation[38] the full Green's function is $G_1^{-1}=G_1^{0-1}-\Sigma$. Using the one-phonon Green's function (A1) for G_1^0, we obtain, rigorously,

$$G_1(Q,\omega)=\frac{2\omega_Q^0}{\omega^2-\omega_Q^{02}-2\omega_Q^0\Sigma_Q(\omega)}. \tag{A7}$$

Writing again $\Sigma_Q(\omega)=\Delta_Q(\omega)-i\Gamma_Q(\omega)$ and defining

$$\omega_Q^2(\omega)\equiv\omega_Q^{02}+2\omega_Q^0\Delta_Q(\omega)\approx[\omega_Q^0+\Delta_Q(\omega)]^2,$$

we have

$$G_1(Q,\omega)=\frac{2\omega_Q^0}{\omega^2-\omega_Q^2+i2\omega_Q^0\Gamma_Q(\omega)} \tag{A8}$$

and

$$A_1(Q,\omega)=\frac{8\omega_Q^{02}\Gamma_Q(\omega)}{[\omega^2-\omega_Q^2(\omega)]^2+[2\omega_Q^0\Gamma_Q(\omega)]^2}. \tag{A9}$$

If Γ_Q is small compared to ω_Q^0 and we again set $\Gamma_Q(\omega)=\Gamma_Q$, we may approximate (A8) by (A4) and (A5) above.[41] Also, following Cochran[42] and Lovesey[41] we may obtain the HO oscillator function (A6) directly from (A9) if we substitute $\omega_Q^0\Gamma_Q(\omega)=\omega\Gamma_Q$ and $\omega_Q(\omega)=\omega_Q$. This definition of Γ_Q is clearly consistent with choosing Γ_Q as the value of $\Gamma_Q(\omega)$ at $\omega=\omega_Q$ and recognizes that $\Gamma_Q(\omega)$ is an odd function of ω. On this basis ω_Q rather than $E_Q=(\omega_Q^2+\Gamma_Q^2)^{1/2}$ represents the excitation energy.

From this discussion, we see that fitting a Lorentzian (A5) or a HO function (A6) will give the same results provided the same excitation energy ω_Q is used. These functions are valid for small Γ_Q. Near T_λ where the response is broad, the frequency dependence of $\omega_Q(\omega)$ and $\Gamma_Q(\omega)$ should be retained and defining a single-particle energy ϵ_Q and inverse lifetime Γ_Q is not meaningful.

*Present address: Department of Physics, University of Keele, Keele, Staffs, ST5 5BG, U.K.

[1]A. D. B. Woods and R. A. Cowley, Rep. Prog. Phys. **36**, 1135 (1973).

[2]D. L. Price, in *The Physics of Liquid and Solid Helium*, edited by K. H. Bennemann and J. B. Ketterson (Wiley, New York, 1978), Vol. II, Chap. 7.

[3]H. R. Glyde, in *Condensed Matter Research Using Neutrons*, edited by S. W. Lovesey and R. Scherm (Plenum, New York, 1984), p. 95.

[4]H. R. Glyde and E. C. Svensson, in *Methods of Experimental Physics*, edited by D. L. Price and K. Sköld (Academic, New York, 1987), Vol. 23, Chap. 13, Part B.

[5]H. Palevsky, K. Otnes, K. E. Larsson, R. Pauli, and R. Stedman, Phys. Rev. **108**, 1346 (1957); H. Palevsky, K. Otnes, and K. E. Larsson, Phys. Rev. **112**, 11 (1958).

[6]J. L. Yarnell, G. P. Arnold, P. J. Bendt, and E. C. Kerr, Phys. Rev. Lett. **1**, 9 (1958); Phys. Rev. **113**, 1379 (1959).

[7]D. G. Henshaw, Phys. Rev. Lett. **1**, 127 (1958).

[8]L. D. Landau, J. Phys. U.S.S.R. **5**, 71 (1941); **11**, 91 (1947).

[9]R. A. Cowley and A. D. B. Woods, Can. J. Phys. **49**, 177 (1971).

[10]O. W. Dietrich, E. H. Graf, C. H. Huang, and L. Passell, Phys. Rev. A **5**, 1377 (1972).

[11]A. D. B. Woods and E. C. Svensson, Phys. Rev. Lett. **41**, 974 (1978).

[12]J. A. Tarvin and L. Passell, Phys. Rev. B **19**, 1458 (1979).

[13]F. Mezei, Phys. Rev. Lett. **44**, 1601 (1980).

[14]F. Mezei and W. G. Stirling, in *75th Jubilee Conference on Helium-4*, edited by J. G. M. Armitage (World Scientific, Singapore, 1983), p. 111.

[15]E. Talbot and A. Griffin, Ann. Phys. (N.Y.) **151**, 71 (1983); Phys. Rev. B **29**, 3952 (1984).

[16]A. Griffin, Phys. Rev. B **19**, 5946 (1979); Phys. Lett. **71A**, 237 (1979); J. Low Temp. Phys. **44**, 441 (1981).

[17]A. Griffin and E. Talbot, Phys. Rev. B **24**, 5075 (1981).

[18]E. Talbot and A. Griffin, Phys. Rev. B **29**, 2531 (1984).

[19]K. Yamada, Prog. Theor. Phys. **63**, 715 (1980).

[20]V. P. Mineev, Pis'ma Zh. Eksp. Teor. Fiz. **32**, 509 (1980) [JETP Lett. **32**, 489 (1980)].

[21]L. D. Landau and I. M. Khalatnikov, Zh. Eksp. Teor. Fiz. **19**, 637 (1949); I. M. Khalatnikov, *An Introduction to the Theory of Superfluidity* (Benjamin, New York, 1965); in Ref. 2, Vol. I, Chap. 1.

[22]S.-K. Ma and C.-W. Woo, Phys. Rev. **159**, 165 (1967); A. Griffin and T. H. Cheung, Phys. Rev. A **7**, 2086 (1973); P. Szèpfalusy and I. Kondor, Ann. Phys. (N.Y.) **82**, 1 (1974); V. K. Wong and H. Gould, *ibid.* **83**, 252 (1974); D. L. Bartley and V. K. Wong, Phys. Rev. B **12**, 3775 (1975), and references therein.

[23]L. Kadanoff and P. Martin, Ann. Phys. (N.Y.) **24**, 419 (1963); P. C. Hohenberg and P. C. Martin, *ibid.* **34**, 291 (1965).

[24]E. C. Svensson, W. G. Stirling, E. Talbot, and H. R. Glyde, in Proceedings of the 18th International Conference on Low Temperature Physics, Kyoto, Japan, 1987 [Jpn. J. Appl. Phys. Suppl. **26**, 33 (1987)].

[25]E. C. Svensson, P. Martel, V. F. Sears, and A. D. B. Woods, Can. J. Phys. **54**, 2178 (1976).

[26]A. Miller, D. Pines, and P. Nozières, Phys. Rev. **127**, 1452 (1962).

[27]A. Griffin, in Proceedings of the Banff International Conference on Quantum Fluids and Solids [Can. J. Phys. **65**, 1368 (1987)].

[28]K. Bedell, D. Pines, and A. Zawadowski, Phys. Rev. B **29**, 102 (1984).

[29]The Landau-Khalatnikov width as calculated at SVP by Bedell, Pines, and Zawadowski (Ref. 28) is well approximated by $\Gamma \simeq 1.14\ \mathrm{T}\ \rho_N(T)/\rho$ (where Γ and T are in the same units) in agreement with Mezei's measurements (Ref. 13). At 24.26 bars, the BPZ calculation gives $\Gamma \simeq 1.2\ \mathrm{T}\ \rho_N(T)/\rho$. We have used $\Gamma^{\mathrm{LK}} = 1.2\ \mathrm{T}\ \rho_N(T)/\rho$ for $p = 20$ bars.

[30]K. Bedell, D. Pines, and I. Fomin, J. Low Temp. Phys. **48**, 417 (1982).

[31]R. Scherm, K. Guckelsberger, B. Fåk, K. Sköld, A. J. Dianoux, H. Godfrin, and W. G. Stirling, Phys. Rev. Lett. **59**, 217 (1989).

[32]E. C. Svensson, V. F. Sears, A. D. B. Woods, and P. Martel, Phys. Rev. B **21**, 3638 (1980); V. F. Sears, E. C. Svensson, A. D. B. Woods, and P. Martel, AECL Report No. AECL-6779, 1979 (unpublished).

[33]R. P. Feynman, Phys. Rev. **94**, 262 (1954).

[34]C. H. Aldrich, III, C. J. Pethick, and D. Pines, J. Low. Temp. Phys. **25**, 691 (1976); D. Pines, in *Highlights of Condensed Matter Theory,* Course 89 of the Varenna Summer School, edited by F. Bassani, F. Fumi, and M. P. Tosi (Soc. Italianna di Fisica, Bologna, Italy, 1985), p. 580.

[35]N. Hugenholtz and D. Pines, Phys. Rev. **116**, 489 (1959); J. Gavoret and P. Nozières, Ann. Phys. (N.Y.) **28**, 349 (1964).

[36]S. H. Payne and A. Griffin, Phys. Rev. B **32**, 7199 (1985); A. Griffin and S. H. Payne, J. Low Temp. Phys. **64**, 155 (1986).

[37]E. C. Svensson and D. C. Tennant, in *Proceedings of the 18th International Conference on Low Temperature Physics,* Kyoto, Japan, 1987, [Jpn. J. Appl. Phys. Suppl. **26**, 31 (1987)].

[38]A. A. Abrikosov, L. P. Gorkov, and I. E. Dzyaloshinski, *Methods of Quantum Field Theory in Statistical Physics* (Prentice Hall, Englewood Cliffs, New Jersey, 1963).

[39]P. Nozières, *The Theory of Interacting Fermi Systems* (Benjamin, New York, 1964), p. 95.

[40]V. Ambegaokar, J. Conway, and G. Baym, in *Lattice Dynamics,* edited by R. F. Wallis (Pergamon, New York, 1965).

[41]S. W. Lovesey, *Theory of Neutron Scattering from Condensed Matter* (Oxford University Press, Oxford, 1984), Vol. I, p. 126 and Appendix B3.

[42]W. Cochran, Adv. Phys. **18**, 157 (1969), Eq. (4.7).